

Cerium(IV), Neptunium(IV), and Plutonium(IV) 1,2-Phenylenediphosphonates: Correlations and Differences between Early Transuranium Elements and Their Proposed Surrogates

Juan Diwu, Shuao Wang, Zuolei Liao, Peter C. Burns, and Thomas E. Albrecht-Schmitt*

Department of Civil Engineering and Geological Sciences and Department of Chemistry and Biochemistry, University of Notre Dame, Notre Dame, Indiana 46556, United States

Received August 6, 2010

The in situ hydrothermal reduction of Np(VI) to Np(IV) and Pu(VI) to Pu(IV) in the presence of 1,2-phenylenediphosphonic acid (**PhP2**) results in the crystallization of $\text{Np}[\text{C}_6\text{H}_4(\text{PO}_3\text{H})_2]_2 \cdot 2\text{H}_2\text{O}$ (**NpPhP2**) and $\text{Pu}[\text{C}_6\text{H}_4(\text{PO}_3\text{H})(\text{PO}_3\text{H}_2)][\text{C}_6\text{H}_4(\text{PO}_3\text{H})(\text{PO}_3)] \cdot 2\text{H}_2\text{O}$ (**PuPhP2**), respectively. Similar reactions have been explored with Ce(IV) resulting in the isolation of the Ce(IV) phenylenediphosphonate $\text{Ce}[\text{C}_6\text{H}_4(\text{PO}_3\text{H})(\text{PO}_3\text{H}_2)][\text{C}_6\text{H}_4(\text{PO}_3\text{H})(\text{PO}_3)] \cdot 2\text{H}_2\text{O}$ (**CePhP2**). Single crystal diffraction studies reveal that although all these three compounds all crystallize in the triclinic space group $P\bar{1}$, only **PuPhP2** and **CePhP2** are isotypic, whereas **NpPhP2** adopts a distinct structure. In the cerium and plutonium compounds edge-sharing dimers of MO_8 polyhedra are bridged by the diphosphonate ligand to create one-dimensional chains. **NpPhP2** also forms chains. However, the NpO_8 units are monomeric. The protonation of the ligands is also different in the two structure types. Furthermore, the NpO_8 polyhedra are best described as square antiprisms (D_{4d}), whereas the CeO_8 and PuO_8 units are trigonal dodecahedra (D_{2d}). Bond-valence parameters of $R_0 = 1.972$ and $b = 0.538$ have been derived for Np^{4+} using a combination of the data reported in this work with that available in crystallographic databases. The UV–vis–NIR absorption spectra of **NpPhP2** and **PuPhP2** are also reported and used to confirm the tetravalent oxidation states.

Introduction

Phosphonates have played a role in actinide partitioning in advanced nuclear fuel cycles.¹ Chelating diphosphonates, and their application to nuclear waste remediation and actinide separation processes, are well-developed.¹ Despite the importance of diphosphonates in actinide separations, little is known about the structural chemistry of actinide

phosphonates other than with U(VI).² In previous reports, we demonstrated that both Np(IV) and Pu(IV) phosphonates and diphosphonates can be prepared via in situ hydrothermal reduction of Np(VI) and Pu(VI), which allows for slow kinetics of crystal growth.^{3–6} This synthetic methodology is broadly applicable to the crystallization of many tetravalent actinide oxoanion systems.^{3–12} In light of this, it is now possible to compare compounds of An^{4+} ($\text{An} = \text{Np}$,

*To whom correspondence should be addressed. E-mail: talbrecl@nd.edu.

(1) (a) Nash, K. L. *J. Alloys Compd.* **1997**, 249, 33. (b) Jensen, M. P.; Beitz, J. V.; Rogers, R. D.; Nash, K. L. *J. Chem. Soc., Dalton Trans.* **2000**, 18, 3058. (c) Chiarizia, R.; Horwitz, E. P.; Alexandratos, S. D.; Gula, M. J. *Sep. Sci. Technol.* **1997**, 32, 1.

(2) (a) Grohol, D.; Clearfield, A. *J. Am. Chem. Soc.* **1997**, 119, 9301. (b) Grohol, D.; Clearfield, A. *J. Am. Chem. Soc.* **1997**, 119, 4662. (c) Grohol, D.; Subramanian, M. A.; Poojary, D. M.; Clearfield, A. *Inorg. Chem.* **1996**, 35, 5264. (d) Aranda, M. A. G.; Cabeza, A.; Bruque, S.; Poojary, D. M.; Clearfield, A. *Inorg. Chem.* **1998**, 37, 1827. (e) Poojary, D. M.; Cabeza, A.; Aranda, M. A. G.; Bruque, S.; Clearfield, A. *Inorg. Chem.* **1996**, 35, 1468. (f) Poojary, D. M.; Cabeza, A.; Aranda, M. A. G.; Bruque, S.; Clearfield, A. *Inorg. Chem.* **1996**, 35, 5603. (g) Poojary, D. M.; Grohol, D.; Clearfield, A. *Angew. Chem., Int. Ed. Engl.* **1995**, 34, 1508. (h) Poojary, D. M.; Grohol, D.; Clearfield, A. *J. Phys. Chem. Solids* **1995**, 56, 1383. (i) Britel, A.; Wozniak, M.; Boivin, J. C.; Nowogrocki, G.; Thomas, D. *Acta Crystallogr.* **1986**, C42, 1502. (j) Grohol, D.; Clearfield, A. *Inorg. Chem.* **1999**, 38, 751. (k) Cabeza, A.; Aranda, M. A. G.; Cantero, F. M.; Lozano, D.; Martínez-Lara; Bruque, S. *J. Solid State Chem.* **1996**, 121, 181. (l) Doran, M. B.; Norquist, A. J.; O'Hare, D. *Chem. Mater.* **2003**, 15, 1449.

(3) Bray, T. H.; Nelson, A.-G. D.; Jin, G. B.; Haire, R. G.; Albrecht-Schmitt, T. E. *Inorg. Chem.* **2007**, 46, 10959.

(4) Nelson, A.-G. D.; Bray, T. H.; Zhan, W.; Haire, R. G.; Albrecht-Schmitt, T. E. *Inorg. Chem.* **2008**, 47, 4945.

(5) Nelson, A.-G. D.; Bray, T. H.; Albrecht-Schmitt, T. E. *Angew. Chem., Int. Ed.* **2008**, 47, 6252.

(6) Nelson, A.-G. D.; Bray, T. H.; Stanley, A. F.; Albrecht-Schmitt, T. E. *Inorg. Chem.* **2009**, 48, 4530.

(7) Diwu, J.; Nelson, A.-G. D.; Albrecht-Schmitt, T. E. *Comments Inorg. Chem.* **2010**, 31, 46.

(8) Diwu, J.; Nelson, A.-G. D.; Wang, S.; Campana, C. F.; Albrecht-Schmitt, T. E. *Inorg. Chem.* **2010**, 49, 3337.

(9) Brandel, V.; Dacheux, N.; Genet, M. *J. Solid State Chem.* **2001**, 159, 139.

(10) Dacheux, N.; Clavier, N.; Wallez, G.; Brandel, V.; Emery, J.; Quarton, M.; Genet, M. *Mater. Res. Bull.* **2005**, 40, 2225.

(11) Dacheux, N.; Clavier, N.; Wallez, G.; Quarton, M. *Solid State Sci.* **2007**, 9, 619.

(12) Dacheux, N.; Grandjean, S.; Rousselle, J.; Clavier, N. *Inorg. Chem.* **2007**, 46, 10390.

Pu) with compounds containing their proposed surrogates (e.g., Ce^{4+} , Zr^{4+} , and Th^{4+}).^{4–8,14–16} Ce^{4+} has been considered as an ideal replacement for tetravalent transuranium elements, especially Pu(IV), owing to their nearly identical ionic radius.¹⁴ We recently prepared and characterized four Pu^{4+} and four Ce^{4+} compounds with methylenediphosphonate as a ligand.^{7,8} Two of the plutonium compounds do not have cerium analogues, and two of the cerium compounds are unique to cerium. While two of the plutonium compounds are isotopic with the cerium phases.

If we ignore the effects of radiolysis, which may not be wise with transuranics, there are still large differences in the redox chemistry of these elements. For instance, Ce^{4+} is the highest oxidation state for cerium, and it is easily reduced to Ce^{3+} ($E^\circ_{\text{Ce(III)/Ce(IV)}} = 1.61$ V/NHE). We established in our previous work that Np^{4+} , which is very difficult to further reduce to Np^{3+} , can be isolated from the precipitation-driven reaction of Np(V) disproportionation.^{3–6} Whereas with Pu^{4+} , which can easily form from the reduction of Pu(VI), the redox potential ($E^\circ_{\text{Pu(III)/Pu(IV)}} = 0.97$ V/NHE) is considerably smaller than its Ce(IV) counterpart.

There is now a considerable body of evidence that demonstrates that surrogates do not properly mimic the behavior of transuranics both in solution⁷ and in the solid-state.^{7–13} For example, the primary hydrolysis product for UO_2^{2+} is a trimer, whereas for PuO_2^{2+} , it is a dimer, which influences how we model these radionuclides in the environment.¹³ Careful examination of the coordination environments of Pu^{4+} and Ce^{4+} with both complex octadentate ligands and simple chelators demonstrates that these two cations can yield substantially different coordination geometries even if they possess the same coordination number.¹⁴ Even rigid extended structures adopt substantially different topologies when U(VI) is replaced by Pu(VI).¹⁸ The largest demonstration of structural differences among actinides and surrogates comes from Dacheux and company, who have carefully reviewed the structural chemistry of tetravalent metal phosphates,^{15–17} and substantial variations can be observed even in dense structures like $\text{M}(\text{PO}_3)_4$ ($\text{M} = \text{Ce}, \text{Th}, \text{U}, \text{Pa}, \text{Np}, \text{Pu}$).¹⁶

Experimental Section

Syntheses. ²⁴²PuO₂ (99.98% isotopic purity, Oak Ridge National Laboratory, $t_{1/2} = 3.76 \times 10^5$ y) was used as received. While the plutonium is of very high isotopic purity, there are trace amounts of ²³⁸Pu, ²⁴⁰Pu, ²⁴¹Pu, ²⁴⁴Pu, and ²⁴¹Am (see Supporting Information, Table 1). The majority of the radioactivity comes from the ²⁴¹Pu even though it represents only 0.008% of the plutonium. **Caution!** ²⁴²Pu still represents a serious health risk owing to its α and γ emission. This isotope was selected because of its long half-life, which increased the longevity of the crystals. ²³⁷NpO₂ (99.9%, Oak Ridge, $t_{1/2} = 2.14 \times 10^6$ y, made

by the oxidation of triple electro-refined Np metal) also represents a serious health risk owing to its α and γ emission. Specialized facilities and procedures are needed for this work. All free-flowing solids are worked with in negative-pressure gloveboxes, and products are only examined when coated with either water or Krytox oil and water. There are some limitations in accurately determining yield with neptunium and plutonium compounds because this requires weighing a dry solid, which poses certain risks as well as manipulation difficulties given the small quantities that we work with.

C₆H₄(PO₃H)₂ (PhP2). 1,2-Bis(dimethoxyphosphoryl)benzene (99%, Alfa Aesar) was dissolved in 20 mL of concentrated hydrochloric acid and heated for 30 min followed by reflux for 8 h. The white crystals of 1,2-phenylenediphosphonic acid (**PhP2**) formed during cooling to room temperature. The crystals were washed with 10 mL of cold hydrochloric acid, filtered, and finally dried in the oven at 60 °C.¹⁹

Ce[C₆H₄(PO₃H)(PO₃H)₂][C₆H₄(PO₃H)(PO₃H)] · 2H₂O (CePhP2). (NH₄)₂Ce(NO₃)₆ (99%, Alfa Aesar) was used as received. (NH₄)₂Ce(NO₃)₆ (0.0525 g, 0.096 mmol) and **PhP2** (0.1291 g, 0.542 mmol) were reacted with 2000 μL of distilled and Millipore filtered water in a 23 mL PTFE autoclave linear. The closed linear was sealed inside a stainless steel autoclave, and then heated to 180 °C for 3 days in a furnace. The furnace was turned off, and the autoclave was allowed to cool to room temperature before opening. The product consisted of colorless acicular crystals of **CePhP2**.

Np[C₆H₄(PO₃H)₂ · 2H₂O (NpPhP2). The stock solution was prepared by first digesting NpO₂ in 8 M HNO₃ for 3 days at 200 °C (in an autoclave). The solution was reduced to a moist residue and redissolved in water forming a Np(VI) nitrate solution. A 50 μL volume of a 0.3717 M stock solution of Np(VI) was placed in an autoclave along with 22.0 mg (0.0092 mmol) of **PhP2** in a 10 mL PTFE autoclave linear. After adding the ligand, the color of the solution changed from pink to green as we observed in the methylenediphosphonate system.⁴ 350 μL of distilled and Millipore filtered water was then added. The closed linear was sealed inside a stainless steel autoclave, and then heated to 180 °C for 3 days in a furnace. The furnace was turned off, and the autoclave was allowed to cool to room temperature before opening. The sole product was green acicular crystals of **NpPhP2**.

Pu[C₆H₄(PO₃H)(PO₃H)₂][C₆H₄(PO₃H)(PO₃H)] · 2H₂O (PuPhP2). The stock solution was prepared by first digesting PuO₂ in 8 M HNO₃ for 3 days at 200 °C (in an autoclave), reduced to a moist residue, and redissolved in water. This solution was then ozonated for approximately 5 h to ensure complete oxidation of the plutonium to +6. UV–vis–NIR spectroscopy indicates that only Pu(VI) is present. A 100 μL volume of a 0.1733 M stock solution of Pu(VI) was placed in an autoclave along with 24.6 mg (0.0103 mmol) of **PhP2** in a 10 mL PTFE autoclave linear inside. A 300 μL volume of distilled and Millipore filtered water was added. The closed linear was sealed inside a stainless steel autoclave, and then heated to 180 °C for 3 days in a furnace. The furnace was turned off, and the autoclave was allowed to cool to room temperature before opening. The product consisted of pale pink acicular crystals of **PuPhP2**, some of which were several millimeters in length, and some amorphous white solid.

Crystallographic Studies. Crystals of all three compounds were mounted on CryoLoops with Krytox oil and optically aligned on a Bruker APEXII Quazar X-ray diffractometer using a digital camera. Initial intensity measurements were performed using a 1 μS X-ray source, a 30 W microfocused sealed tube (MoK α , $\lambda = 0.71073$ Å) with high-brilliance and high-performance focusing Quazar multilayer optics. Standard APEXII software was used for determination of the unit cells and data collection control. The intensities of reflections of a sphere were collected by a combination of four sets of exposures (frames).

(13) Reilly, S. D.; Neu, M. P. *Inorg. Chem.* **2006**, *45*, 1839.

(14) (a) Gorden, A. E. V.; Shuh, D. K.; Tiedemann, B. E. F.; Wilson, R. E.; Xu, J.; Raymond, K. N. *Chemistry* **2005**, *11*, 2842. (b) Gorden, A. E. V.; Xu, J.; Raymond, K. N. *Chem. Rev.* **2003**, *103*, 4207. (c) Xu, J.; Radkov, E.; Ziegler, M.; Raymond, K. N. *Inorg. Chem.* **2000**, *39*, 4156. (d) Szigethy, G.; Xu, J.; Gorden, A. E. V.; Teat, S. J.; Shuh, D. K.; Raymond, K. N. *Eur. J. Inorg. Chem.* **2008**, *13*, 2143.

(15) Brandel, V.; Dacheux, N. *J. Solid State Chem.* **2004**, *177*, 4743.

(16) Brandel, V.; Dacheux, N. *J. Solid State Chem.* **2004**, *177*, 4755.

(17) Dacheux, N.; Podor, R.; Brandel, M.; Genet, M. *J. Nucl. Mater.* **1998**, *252*, 179–186.

(18) (a) Runde, W.; Bean, A. C.; Albrecht-Schmitt, T. E.; Scott, B. L. *Chem. Commun.* **2003**, *4*, 478. (b) Bean, A. C.; Scott, B. L.; Albrecht-Schmitt, T. E.; Runde, W. *Inorg. Chem.* **2003**, *42*, 5632.

(19) Reiter, S. A.; Assmann, B.; Nogai, S. D.; Mitzel, N. W.; Schmidbaur, H. *Helv. Chim. Acta* **2002**, *85*, 1140.

Table 1. Crystallographic Data for Ce[C₆H₄(PO₃H)(PO₃H₂)] [C₆H₄(PO₃H)(PO₃H₂)]·2H₂O (**CePhP2**), Np[C₆H₄(PO₃H₂)₂]·2H₂O (**NpPhP2**), Pu[C₆H₄(PO₃H)(PO₃H₂)] [C₆H₄(PO₃H)(PO₃H₂)]·2H₂O (**PuPhP2**)

compound	CePhP2	NpPhP2	PuPhP2
formula mass	644.22	741.10	746.10
color and habit	colorless, acicular	pale-green, acicular	pink, acicular
space group	<i>P</i> $\bar{1}$ (No. 2)	<i>P</i> $\bar{1}$ (No. 2)	<i>P</i> $\bar{1}$ (No. 2)
<i>a</i> (Å)	9.467(1)	7.886(1)	9.444(3)
<i>b</i> (Å)	10.044(1)	9.863(1)	10.021(3)
<i>c</i> (Å)	12.671(2)	12.810(2)	12.670(3)
α (deg)	74.042(2)	100.644(2)	74.024(2)
β (deg)	78.299(2)	95.617(2)	78.452(2)
γ (deg)	65.809(1)	102.669(1)	66.042(2)
<i>V</i> (Å ³)	1051.1(2)	945.3(2)	1048.1(5)
<i>Z</i>	2	2	2
<i>T</i> (K)	100(2)	100(2)	100(2)
λ (Å)	0.71073	0.71073	0.71073
maximum 2θ (deg.)	28.81	27.49	27.50
ρ_{calcd} (g cm ⁻³)	2.035	2.604	2.364
μ (Mo <i>K</i> α) (cm ⁻¹)	25.38	59.11	35.19
<i>R</i> (<i>F</i>) for $F_o^2 > 2\sigma(F_o^2)^a$	0.0409	0.0280	0.0257
<i>R</i> _w (F_o^2) ^b	0.0871	0.0773	0.0679

$$^a R(F) = \sum ||F_o| - |F_c|| / \sum |F_o|. \quad ^b R_w(F_o^2) = [\sum w(F_o^2 - F_c^2)^2 / \sum wF_o^4]^{1/2}.$$

Each set had a different ϕ angle for the crystal, and each exposure covered a range of 0.5° in ω . A total of 1464 frames were collected with an exposure time per frame of 10 to 50 s, depending on the crystal. SAINT software was used for data integration including Lorentz and polarization corrections. Semiempirical absorption corrections were applied using the program SADABS.²⁰ Selected crystallographic information is listed in Table 1. Atomic coordinates and additional structural information are provided in the Supporting Information (CIFs).

UV-vis-NIR Spectroscopy. UV-vis-NIR data were acquired from single crystals using a Craic Technologies microspectrophotometer. Crystals were placed on quartz slides under Krytox oil, and the data were collected from 400 to 1500 nm. The exposure time was auto optimized by the Craic software.

Results and Discussion

Synthesis. **PhP2** does not react directly with PuO₂, whereas the reactions with a Pu(VI) solution yielded high quality pale pink crystals after hydrothermal treatment. The reactivity of **PhP2** sharply contrasts with methylenediphosphonic acid in that the latter directly reacts with PuO₂ to yield crystalline Pu(IV) compounds.^{6,8} The redox potentials for Ce⁴⁺/Ce³⁺, Np⁶⁺/Np⁴⁺, and Pu⁶⁺/Pu⁴⁺ are 1.61, 0.88, and 0.936 V/NHE, respectively. In the **PhP2** system, Ce⁴⁺ retains its oxidation state, whereas Np(VI) and Pu(VI) are reduced to +4 oxidation states. On the basis of the reduction potentials, it would have been predicted that Ce(IV) should have been reduced to Ce(III). These observations indicate that the formation of these products is solubility-driven. The tetravalent cations, U⁴⁺, Np⁴⁺, and Pu⁴⁺ yield solids that are typically many orders of magnitude less soluble than compounds formed with UO₂²⁺, NpO₂²⁺, and PuO₂²⁺. Therefore, the reduction processes for Np(VI) and Pu(VI) are being driven in part by the formation of solids of low solubility. Apparently the Ce(IV) compound precipitates before reduction can take place.

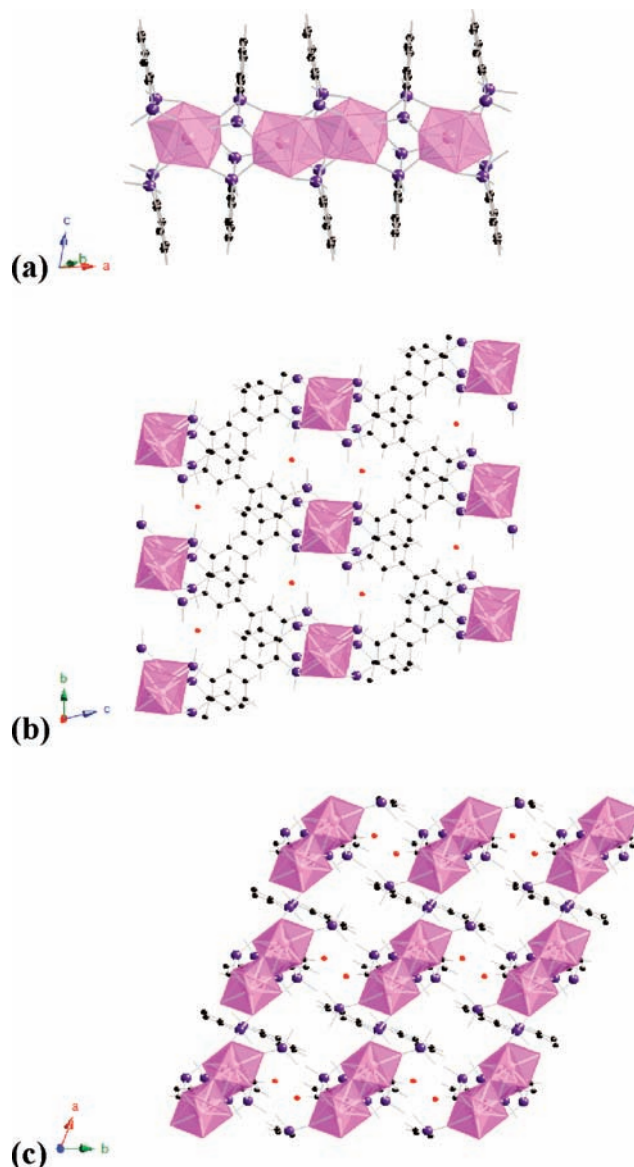


Figure 1. Depiction of the one-dimensional structure of M[C₆H₄(PO₃H)(PO₃H₂)] [C₆H₄(PO₃H)(PO₃H₂)]·2H₂O (M = Ce⁴⁺, Pu⁴⁺). (a) In-sights into the coordination environment of the MO₈. (b) Relative overlap of the positions of the phenyl groups along the *a* axis. (c) Arrangement of the MO₈ dimers.

Crystal Structures of CePhP2 and PuPhP2. **CePhP2** and **PuPhP2** are isotypic and form one-dimensional chains where the M(IV) (M = Ce, Pu) centers are coordinated by 1,2-phenylenediphosphonic acid (**PhP2**). Figure 1a shows the depiction of the chains that extend along the *a* axis. The metal centers are eight coordinate with **PhP2** not only bridging but also chelating the centers via the PO₃ moieties. The phenyl rings extend into the space between the chains. The MO₈ polyhedra share an edge to form dimers within the chains. Six **PhP2** moieties are bound to each dimer. Four of these bridge between the dimers to form the infinite chains. The two PO₃ moieties that belong to the same phenyl ring coordinate the metal centers differently. The two ligands that are a part of the dimer itself also chelate the M(IV) centers. When **PhP2** chelates, the PO₃ unit of one **PhP2** moiety chelates to one metal center while the other PO₃ unit from the same **PhP2**

(20) Sheldrick, G. M. *SADABS, Program for absorption correction using SMART CCD based on the method of Blessing*. Blessing, R. H. *Acta Crystallogr.*, **1995**, *A51*, 33.

(21) Roulhac, P. L.; Palenik, G. J. *Inorg. Chem.* **2003**, *42*, 118.

(22) Kepert, D. L. *Prog. Inorg. Chem.* **1978**, *24*, 179.

(23) Brese, N. E.; O'Keeffe, M. *Acta Crystallogr.* **1991**, *B47*, 192.

Table 2. Selected Bond Distances (Å) for $\text{Ce}[\text{C}_6\text{H}_4(\text{PO}_3\text{H})(\text{PO}_3\text{H}_2)][\text{C}_6\text{H}_4(\text{PO}_3\text{H})(\text{PO}_3)] \cdot 2\text{H}_2\text{O}$ (**CePhP2**)

Bond Distances (Å)			
Ce(1)–O(1)	2.320(3)	P(2)–O(4)	1.533(3)
Ce(1)–O(4)	2.225(3)	P(2)–O(5)	1.500(3)
Ce(1)–O(5)	2.293(3)	P(2)–O(6)	1.555(3)
Ce(1)–O(7)	2.340(3)	P(2)–C(2)	1.797(5)
Ce(1)–O(8)	2.295(3)	P(3)–O(7)	1.521(3)
Ce(1)–O(10)	2.375(3)	P(3)–O(8)	1.509(3)
Ce(1)–O(10)'	2.541(3)	P(3)–O(9)	1.556(3)
Ce(1)–O(11)	2.296(3)	P(3)–C(7)	1.813(5)
P(1)–O(1)	1.496(3)	P(4)–O(10)	1.536(3)
P(1)–O(2)	1.565(3)	P(4)–O(11)	1.535(3)
P(1)–O(3)	1.546(4)	P(4)–O(12)	1.511(3)
P(1)–C(1)	1.801(5)	P(4)–C(8)	1.802(5)

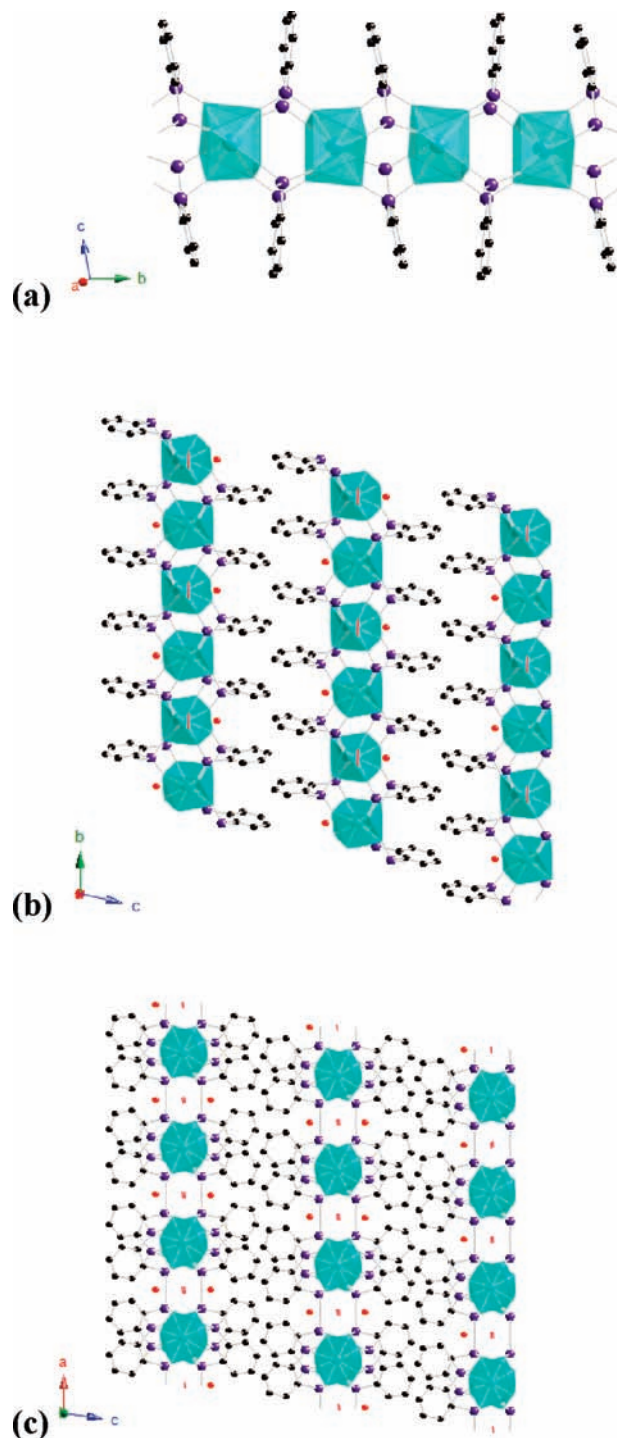
Table 3. Selected Bond Distances (Å) for $\text{Np}[\text{C}_6\text{H}_4(\text{PO}_3\text{H})_2]_2 \cdot 2\text{H}_2\text{O}$ (**NpPhP2**)

Bond Distances (Å)			
Np(1)–O(1)	2.321(4)	P(2)–O(4)	1.505(4)
Np(1)–O(2)	2.273(3)	P(2)–O(5)	1.521(4)
Np(1)–O(4)	2.316(3)	P(2)–O(6)	1.561(4)
Np(1)–O(5)	2.450(3)	P(2)–C(2)	1.812(5)
Np(1)–O(7)	2.279(3)	P(3)–O(7)	1.504(4)
Np(1)–O(8)	2.299(3)	P(3)–O(8)	1.507(4)
Np(1)–O(10)	2.457(3)	P(3)–O(9)	1.568(4)
Np(1)–O(11)	2.325(3)	P(3)–C(8)	1.796(5)
P(1)–O(1)	1.516(4)	P(4)–O(10)	1.522(4)
P(1)–O(2)	1.501(4)	P(4)–O(11)	1.503(4)
P(1)–O(3)	1.574(4)	P(4)–O(12)	1.558(4)
P(1)–C(1)	1.798(5)	P(4)–C(7)	1.811(5)

bridges between the two metal centers. The second **PhP2** ligand behaves in a similar fashion, but only chelates the metal center that was not chelated by the first **PhP2** moiety. Figure 1b and Figure 1c show the overlap of the phenyl groups and the arrangement of the dimers in space with the two cocrystallized water molecules. There are hydrogen bondings in both structures. Bond-valence sum calculation confirms the presence of Ce^{4+} .²¹ The average bond distances of Ce and Pu are 2.336(4) Å and 2.331(3) Å, respectively. Therefore there are no measurable differences between the Pu–O bonds and Ce–O bonds (Tables 2 and 4).

Crystal Structure of NpPhP2. The structure of **NpPhP2** is also a one-dimensional chain structure. Figure 2a shows the depiction of the monomer chains that extend along the *b* axis. The NpO_8 units are formed by 1,2-phenylenediphosphonic acid (**PhP2**) only bridging between two adjacent metal centers. Each NpO_8 is surrounded by eight PO_3 moieties from four **PhP2** groups. Figure 2b and Figure 2c illustrate the interaction of the phenyl rings and the arrangement of the chains in the space with two free water molecules. The red line in the figures are disordered water molecules. A hydrogen bonding network exists. However, the disorder of the cocrystallized water molecule makes illustrating this network difficult. The average bond distance for **NpPhP2** is 2.340(3) Å, which might be considered as being slightly larger than **PuPhP2**, and might be consistent with the actinide contraction, though this difference is almost not statistically significant. The selected bond distances are given in Table 3.

Comparison of Ce, Pu, and Np Compounds. The differences between the Ce, Pu, and Np structures extend beyond the presence of dimers and monomers. The geometries around the MO_8 polyhedra are in fact quite different. Using

**Figure 2.** Depiction of the one-dimensional structure of $\text{Np}[\text{C}_6\text{H}_4(\text{PO}_3\text{H})_2]_2 \cdot 2\text{H}_2\text{O}$. (a) Insight into the coordination environment of the NpO_8 . (b) Relative overlap of the position of the phenyl groups along the *b* axis. (c) Arrangement of the NpO_8 monomers.

the algorithm developed by Raymond and co-workers,^{14b} we probed the coordination environments around the metal centers. The dihedral angles of all the adjacent faces are calculated and compared with the ideal angles from the three possible distortions of a dodecahedron (D_{4d} , D_{2d} , and C_{2v}). The Kepert ligand repulsion model with $n = 8$ is utilized.²² The evaluation of the calculation is the standard deviation of the dihedral angles along all edges. The results are shown in Table 5. The Ce and Pu are very close to being D_{2d} , which is

Table 4. Selected Bond Distances (Å) for Pu[C₆H₄(PO₃H)(PO₃H₂)](C₆H₄(PO₃H)(PO₃)]·2H₂O (PuPhP2)

Bond Distances (Å)			
Pu(1)–O(1)	2.295(3)	P(2)–O(4)	1.523(3)
Pu(1)–O(4)	2.235(3)	P(2)–O(5)	1.505(3)
Pu(1)–O(5)	2.276(3)	P(2)–O(6)	1.554(3)
Pu(1)–O(7)	2.285(3)	P(2)–C(2)	1.805(5)
Pu(1)–O(8)	2.338(3)	P(3)–O(7)	1.520(3)
Pu(1)–O(10)	2.365(3)	P(3)–O(8)	1.518(3)
Pu(1)–O(10)	2.562(3)	P(3)–O(9)	1.556(3)
Pu(1)–O(12)	2.290(3)	P(3)–C(7)	1.810(5)
P(1)–O(1)	1.494(3)	P(4)–O(10)	1.539(4)
P(1)–O(2)	1.538(4)	P(4)–O(11)	1.512(3)
P(1)–O(3)	1.565(4)	P(4)–O(12)	1.537(3)
P(1)–C(1)	1.805(5)	P(4)–C(8)	1.803(5)

Table 5. Shape Calculation of the Eight Coordinate Polyhedra

element	D_{4d}	C_{2v}	D_{2d}
Ce	16.2287	11.9575	4.1933
Np	3.4442	14.2422	15.5381
Pu	16.4146	12.2319	4.3750

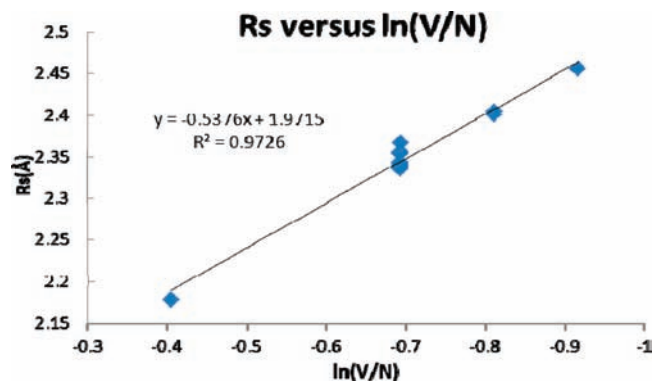
Table 6. Bond-Valence Sum Comparison for CePhP2, NpPhP2, and PuPhP2

	CePhP2		NpPhP2		PuPhP2	
	P–O bond distance	bond valence	P–O bond distance	bond valence	P–O bond distance	bond valence
O1	1.496	1.845	1.516	1.791	1.494	1.886
O2	1.565	1.111	1.501	1.892	1.538	1.195
O3	1.546	1.170	1.574	1.084	1.565	1.111
O4	1.533	1.866	1.505	1.834	1.523	1.867
O5	1.500	1.869	1.521	1.663	1.505	1.872
O6	1.555	1.143	1.561	1.123	1.554	1.145
O7	1.521	1.732	1.504	1.875	1.52	1.808
O8	1.509	1.834	1.507	1.844	1.518	1.749
O9	1.556	1.139	1.568	1.102	1.556	1.138
O10	1.536	1.916	1.522	1.654	1.539	1.936
O11	1.535	1.745	1.503	1.833	1.512	1.282
O12	1.511	1.286	1.558	1.132	1.537	1.745

trigonal dodecahedron, whereas the Np is close to being D_{4d} , a square antiprism.

The protonation of the ligands is also different in the two structure types. Here we calculated the bond-valence sum of the oxygen atoms in each compound, and the results are given in Table 6 (Supporting Information, Tables 2, 3, and 4).^{8,21,25} In CePhP2 and PuPhP2, O(2), O(3), O(6), and O(9) are protonated as indicated by the Bond-Valence Sum (BVS). Even though the BVS of O(12) is very close to 1, the short bond distance demonstrates that it is a terminal P=O unit. This is why the formula of MPhP2 (M = Ce, Pu), $M[C_6H_4(PO_3H)(PO_3H_2)][C_6H_4(PO_3H)(PO_3)] \cdot 2H_2O$, is expressed differently from NpPhP2 even though it involves the same number of protons. The ligand in the former compounds has three ways to bond to the metal center, chelating, bridging, and terminating. For NpPhP2, only O(3), O(6), O(9), and O(12) are protonated, meaning in each PhP2 unit only one PO₃ moiety is actually PO₃H. The ligand here, as we discussed in the structure description, only bridges between the monomers to extend the chains. This singular method of binding the Np centers results in higher symmetry at the metal center versus the Ce and Pu compounds.

Bond-Valence Parameters for Neptunium(IV). While Np(IV) structures are sparse, the structures available in

**Figure 3.** Plot of R_s , the average Np–O bond distance of each compound, versus $\ln(V/N)$, yielding bond-valence parameters of $b = 0.538$ and $R_0 = 1.972$.

crystallographic databases with the addition of the NpPhP2 provide enough data to determine the bond-valence parameters for Np(IV).^{24–27} Using the following equations,^{28,29} we derived the bond-valence parameters for Np(IV) using the structures available in ICSD combined with the data presented in this paper.

$$S = \exp((R_0 - R)/b) \quad (1)$$

$$R_s = R_0 - b \ln(S) \quad (2)$$

R_s is the measured bond distance, which is calculated as the average Np–O bond distance of each compound, and S is the bond-valence that corresponds to this distance. S is calculated using V/N ; where V is the ionic charge, which is treated as the same as the formal oxidation state, and N is the coordination number. Although there are seventeen Np⁴⁺ crystals in the ICSD, as shown in Table 7,³⁰ not all of these are of sufficient quality to be used for bond-valence calculations (those with * are used). On the basis

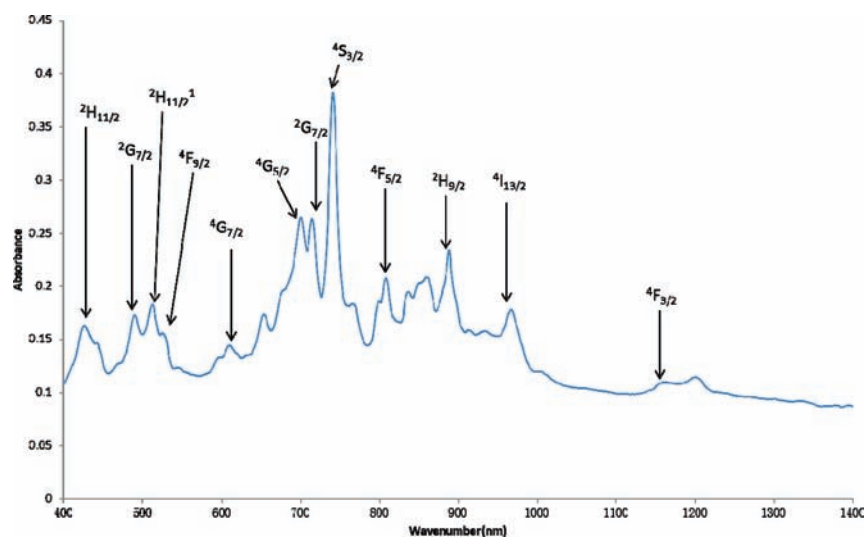
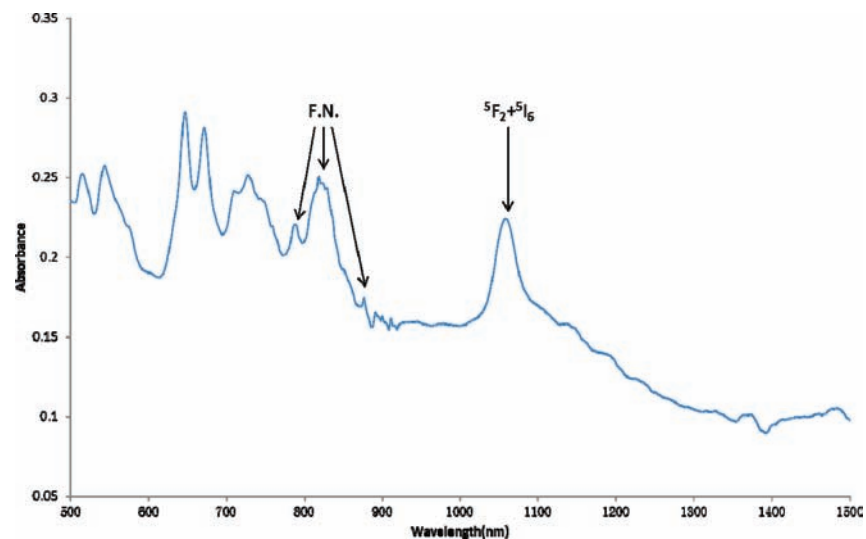
(24) Brown, I. D. *Acta Crystallogr.* **1977**, *B33*, 1305.(25) Brown, I. D. *Acta Crystallogr.* **1992**, *B48*, 553.(26) Brown, I. D. *The Chemical Bond in Inorganic Chemistry. The Bond Valence Model*; Oxford University Press: New York, 2002.(27) Sidey, V. *Acta Crystallogr.* **2009**, *B65*, 401.(28) Burns, P. C. *Can. Mineral.* **1997**, *35*, 1551.(29) Brown, I. D. *Acta Crystallogr.* **2009**, *B65*, 684.

(30) ICSD codes: (a) 8208:Tabuteau, A.; Cousson, A.; Pages, M. *Acta Crystallogr.* **1979**, *B35*, 2000. (b) 31725:Zachariassen, W. H. *Acta Crystallogr.* **1949**, *2*, 388. (c) 600568:Benedict, U.; Dabos, S.; Dufour, C.; Spirlet, J. C.; Pages, M. *J. Less-Common Met.* **1986**, *121*, 461. (d) 647172:Asprey, L. B.; Ellinger, F. H.; Fried, S.; Zachariassen, W. H. *J. Am. Chem. Soc.* **1955**, *77*, 1707. (e) 647174:Lander, G. H.; Mueller, M. H. *Phys. Rev. B* **1974**, *10*, 1994. (f) 647175:Sudakov, L. V.; Kapshukov, I. I.; Solntsev, V. M. *Sov. Atomic Energy* **1973**, *35*, 751. (g) 647176:Taylor, D. *Trans. J. British Cer. Soc.* **1984**, *83*, 32. (h) 41043:Cousson, A.; Abazli, H.; Nectoux, F.; Jove, J.; Pages, M. *J. Less-Common Met.* **1986**, *121*, 405. (i) 61316: Keller, C. *Kern. Karlsruhe: Bericht* **1964**, *225*, 29. (j) 85338:Charushnikova, I. A.; Gamov, A. Yu.; Krot, N. N.; Katsner, S. B. *Radiokhim.* **1997**, *39*, 423. (k) 89421: Charushnikova, I. A.; Krot, N. N.; Starikova, Z. A. *Radiokhim.* **1999**, *41*, 104. (l) 92109:Charushnikova, I. A.; Krot, N. N.; Starikova, Z. A. *Radiokhim.* **2000**, *42*, 36. (m) 92110:Charushnikova, I. A.; Krot, N. N.; Starikova, Z. A. *Radiokhim.* **2000**, *42*, 40. (n) 92111:Charushnikova, I. A.; Krot, N. N.; Starikova, Z. A. *Radiokhim.* **2000**, *42*, 40. (o) 109753:Grigor'ev, M. S.; Charushnikova, I. A.; Krot, N. N.; Yanovskii, A. I.; Struchkov, Y. T. *Radiokhim.* **1997**, *39*, 419. (p) 151319:Hauck *J. Inorg. Nucl. Chem. Lett* **1976**, *12*, 617. (q) 173369:Bray, T. H.; Nelson, A.-G. D.; Jin, G. B.; Haire, R. G.; Albrecht-Schmitt, T. E. *Inorg. Chem.* **2007**, *46*, 10959. (r) 249468&249469:Bray, T. H.; Ling, J.; Choi, E. S.; Brooks, J. S.; Beitz, J. V.; Sykora, R. E.; Haire, R. G.; Stanbury, D. M.; Albrecht-Schmitt, T. E. *Inorg. Chem.* **2007**, *46*, 3663. (s) 249669:Nelson, A.-G. D.; Bray, T. H.; Zhan, W.; Haire, R. G.; Albrecht-Schmitt, T. E. *Inorg. Chem.* **2008**, *47*, 4945. (t) 281697:Almond, P. M.; Sykora, R. E.; Skanthakumar, S.; Soderholm, L.; Albrecht-Schmitt, T. E. *Inorg. Chem.* **2004**, *43*, 958. (u) 419434:Nelson, A.-G. D.; Bray, T. H.; Albrecht-Schmitt, T. E. *Angew. Chem., Int. Ed.* **2008**, *47*, 6252.

Table 7. Results from the Calculations of Bond-Valence Parameters for Np(IV)^a

name	CN	R	S	ICSD
Np(VO ₃) ₄	7	2.321	4.19	8208 ^{30a}
NpO ₂ *	8	2.354	3.93	31725, ^{30b} 600568, ^{30c} 647172, ^{30d} 647174, ^{30e} 647175, ^{30f} 647176 ^{30g}
(NH ₄)Np(OH) ₅	9	2.314	4.79	41043 ^{30h}
BaNpO ₃ *	6	2.178	4.08	61316 ³⁰ⁱ
K ₄ Na ₃ H[Np(W ₅ O ₁₈) ₂](H ₂ O) ₁₆ *	8	2.342	4.02	85338 ^{30j}
K _{5.5} (H ₅ O ₂) _{0.5} Np(SO ₄) ₅ (H ₂ O)*	10	2.454	4.11	89421 ^{30k}
Na ₁₀ Np ₂ (SO ₄) ₉ (H ₂ O) ₄	9	2.400	4.10	92109 ^{30l}
Np(SO ₄) ₂ (H ₂ O) ₄ *	8	2.335	4.08	92110 ^{30m}
Cs ₂ Np(SO ₄) ₃ (H ₂ O) ₂ *	9	2.405	4.05	92111 ³⁰ⁿ
Np(C ₂ O ₄) ₂ (H ₂ O) ₆	8	2.454	3.28	109753 ^{30o}
Np(HCOO) ₄	8	2.493	3.05	151319 ^{30p}
Np(CH ₃ PO ₃)(CH ₃ PO ₃ H)* (NO ₃)(H ₂ O) ₂ *	8	2.354	4.07	173369 ^{30q}
Np(IO ₃) ₄ *	8	2.344	4.01	249468 ^{30r}
Np(IO ₃) ₄ (HIO ₃) _{0.03} (H ₂ O) _{0.91} *	9	2.400	4.13	249469 ^{30r}
Np((CH ₂ (PO ₃) ₂)(H ₂ O) ₂ *)	8	2.367	3.98	249669 ^{30s}
Np(NpO ₂) ₂ (SeO ₃) ₃ *	8	2.356	3.93	281697 ^{30t}
UO ₂ Np(H ₂ O) ₂ * (CH ₂ (PO ₃)(PO ₃ H)) ₂ *	8	2.338	4.11	419434 ^{30u}
Np[C ₆ H ₄ (PO ₃ H) ₂] ₂ ·2(H ₂ O)*	8	2.340	4.07	this work

^a CN = coordination number; R = bond distance average; S = bond-valence sum; ICSD = Inorganic Crystal Structural Database.

**Figure 4.** UV-vis-NIR spectra of light green acicular crystals of Np[C₆H₄(PO₃H)₂]₂·2H₂O showing the assigned peaks for different f-f transitions.**Figure 5.** UV-vis-NIR spectra of pale pink acicular crystals of Pu[C₆H₄(PO₃H)(PO₃H₂)] [C₆H₄(PO₃H)(PO₃)]·2H₂O showing the assigned peaks for different f-f transitions (at wavelengths < 909 nm, multiple J values contribute).

of these data, a plot of R_s versus $\ln(S)$ was generated, as shown in Figure 3. This straight line has a slope of -0.538 and intercept 1.972 ($R^2 = 0.9726$), yielding $b = 0.538$ and $R_o = 1.972$. The results of the bond-valence sums using eq 1 for each compound are also shown in Table 7, and indicate that these parameters fit for most of the compounds.

UV-vis-NIR Spectroscopy. The UV-vis-NIR spectra of **NpPhP2** and **PuPhP2** were collected from single crystals using a microspectrophotometer. Np^{4+} and Pu^{4+} compounds yield characteristic absorption features that consist of a series of Laporte-forbidden f-f transitions.^{8,31-36} These transitions have been assigned throughout the UV-vis-NIR spectrum for Np^{4+} . However, with Pu^{4+} multiple J states contribute at wavelengths shorter than 909 nm. The spectra and assignment for **NpPhP2** and **PuPhP2** are provided in Figures 4 and 5. Both confirm that the compounds are in +4 oxidation states.

Conclusions

Our previous comparisons of Pu(IV) and Ce(IV) diphosphonates yielded a series of compounds where similar, but not identical, MO_7 coordination environments are adopted by the metal centers.^{7,8} In the compounds reported in this work the metal centers expand their coordination environments to more typical MO_8 polyhedra. The Ce(IV) and Pu(IV) compounds are isotypic, and both have trigonal dodecahedral geometries around the metal centers. The expansion in ionic radius expected upon changing Pu(IV) to Np(IV) is on the order of 0.01 Å. This expansion is detected in the bond distances when Np(IV) is compared to Pu(IV), but more importantly the MO_8 units are no longer approxi-

mated by a trigonal dodecahedron but rather by a square antiprism. This local change is reflected in gross changes in the structures. In the Ce/Pu structure type, dimers of edge-sharing MO_8 units are formed; whereas these dimers do not exist in the Np compound, and the ligand functions in several binding modes in the Ce/Pu compounds, whereas in the Np compound there is a single coordination feature. All three compounds are one-dimensional, and this differentiates this group of compounds from those with methylenediphosphonate, all of which adopted three-dimensional networks.⁴⁻⁸ We repeated the syntheses of these compounds under identical conditions to determine if pH or stoichiometry were responsible for different compounds forming, and the results were the same as reported herein. This strongly suggests that there are inherent differences between the chemistry of the tetravalent actinides with diphosphonates as ligands. Perhaps the most important experiment was mixing equal molar ratios of Np(VI) and Pu(VI) in the same reaction. This yields $\text{Np}[\text{C}_6\text{H}_4(\text{PO}_3\text{H})_2]_2 \cdot 2\text{H}_2\text{O}$ (**NpPhP2**) and $\text{Pu}[\text{C}_6\text{H}_4(\text{PO}_3\text{H})(\text{PO}_3\text{H}_2)][\text{C}_6\text{H}_4(\text{PO}_3\text{H})(\text{PO}_3)] \cdot 2\text{H}_2\text{O}$ (**PuPhP2**) rather than a single product containing disordered actinides. Whether this is a reflection of the change in ionic radius or the result of the compounds crystallizing at different times is unknown. However, it provides clear indication of two neighboring actinides displaying very different chemistry.

Acknowledgment. We are grateful for support provided by the Chemical Sciences, Geosciences, and Biosciences Division, Office of Basic Energy Sciences, Office of Science, Heavy Elements Program, U.S. Department of Energy, under Grant DE-FG02-01ER16026 and DE-SC0002215. This material is based upon work supported as part of the Materials Science of Actinides, an Energy Frontier Research Center funded by the U.S. Department of Energy, Office of Science, Office of Basic Energy Sciences under Award Number DE-SC0001089.

Supporting Information Available: X-ray crystallographic files for $\text{Ce}[\text{C}_6\text{H}_4(\text{PO}_3\text{H})(\text{PO}_3\text{H}_2)][\text{C}_6\text{H}_4(\text{PO}_3\text{H})(\text{PO}_3)] \cdot 2\text{H}_2\text{O}$ (**CePhP2**), $\text{Np}[\text{C}_6\text{H}_4(\text{PO}_3\text{H})_2]_2 \cdot 2\text{H}_2\text{O}$ (**NpPhP2**), $\text{Pu}[\text{C}_6\text{H}_4(\text{PO}_3\text{H})(\text{PO}_3\text{H}_2)][\text{C}_6\text{H}_4(\text{PO}_3\text{H})(\text{PO}_3)] \cdot 2\text{H}_2\text{O}$ (**PuPhP2**). This material is available free of charge via the Internet at <http://pubs.acs.org>.

(31) Du Fou de Kerdaniel, E.; Clavier, N.; Dacheux, N.; Terra, O.; Podor, R. *J. Nucl. Mater.* **2007**, *362*, 451-458.

(32) Carnall, W. T.; Liu, G. K.; Williams, C. W.; Reid, M. F. *J. Chem. Phys.* **1991**, *95*, 7194.

(33) Clark, D. L.; Conradson, S. D.; Keogh, D. W.; Palmer, P. D.; Scott, B. L.; Tait, C. D. *Inorg. Chem.* **1998**, *37*, 2893.

(34) Kim, J. I.; Lierse, C.; Baumgartner, F. ACS Symposium Series; American Chemical Society: Washington, DC, 1983; No. 216, p 317.

(35) Eiswirth, M.; Kim, J. I.; Lierse, C. *Radiochim. Acta* **1985**, *38*, 1971.

(36) Capdevila, H.; Vitorge, P.; Giffaut, E.; Delmau, L. *Radiochim. Acta* **1996**, *93*.